

This is the accepted manuscript made available via CHORUS. The article has been published as:

Comment on “Magnetotransport signatures of a single nodal electron pocket constructed from Fermi arcs”

Sudip Chakravarty and Zhiqiang Wang

Phys. Rev. B **96**, 146501 — Published 12 October 2017

DOI: [10.1103/PhysRevB.96.146501](https://doi.org/10.1103/PhysRevB.96.146501)

Comment on “Magnetotransport signatures of a single nodal electron pocket constructed from Fermi arcs”

Sudip Chakravarty and Zhiqiang Wang

Department of Physics and Astronomy, University of California Los Angeles, Los Angeles, California 90095-1547

We comment on the recent work [N. Harrison, *et al.* Phys. Rev. B **92**, 224505 (2015)] which attempts to explain the sign reversal and quantum oscillations of the Hall coefficient observed in cuprates from a single nodal diamond-shaped electron pocket with concave arc segments. Given the importance of this work, it calls for a closer scrutiny. Their conclusion of sign reversal of the Hall coefficient depends on a non-generic rounding of the sharp vertices. Moreover, their demonstration of quantum oscillation in the Hall coefficient from a single pocket is unconvincing. We maintain that at least two pockets with different scattering rates is necessary to explain the observed quantum oscillations of the Hall coefficient.

I. INTRODUCTION

In a recent work,¹ N. Harrison and S. E. Sebastian have drawn attention to the high- T_c community of an intriguing idea. They have suggested that the sign reversal of the Hall coefficient and its quantum oscillations by making a reconstructed version of the observed Fermi arcs into a single diamond shaped electron pocket shown in Fig 1. The problem is that any natural reconstruction leads to both electron and hole-like pockets.

The nodal Fermi arcs observed in an underdoped cuprate are pieced together to a single diamond-shaped electron pocket centered at the nodal point $(k_x, k_y) = (\frac{\pi}{2}, \frac{\pi}{2})$ of the Brillouin zone, although we do not have an understanding of the Fermi arcs themselves. Given this lack of understanding, the construction by a simple shift of the wave vector needs to be understood in some depth. Be that as it may, we address the simpler aspects assuming that this process can be justified in the future. This electron pocket has four concave arcs with sharp vertices, as schematically reproduced in Fig 1. Assuming that the magnitude of the velocity is a constant over the whole Fermi surface contour and ignoring any rounding of the sharp vertices, they have been able to compute the magnetic field- B -dependent conductivities σ_{xx} and σ_{xy} by using the semi-classical Shockley-Chambers formula^{2,3}. Then, from σ_{xx} and σ_{xy} , the Hall coefficient R_H can be derived. This treatment follows exactly Ref. 4. In Ref. 1 Harrison and Sebastian have found that if each side of the diamond pocket is sufficiently concave, which means the angle α in Fig 1 is large enough, the Hall coefficient R_H changes its sign from being positive at $B = 0$ to negative at high fields, which can potentially explain the sign reversal of Hall coefficient¹ as a function of temperature observed in experiments⁵.

To explain the quantum oscillations observed in R_H ⁶, the authors in Ref. 1 made the following substitution for the mean free time τ in the Chambers formula:

$$\tau^{-1} \rightarrow \tilde{\tau}^{-1} \equiv [1 + 2 \cos(2\pi F/H - \pi) e^{-\pi/\omega_c \tau}] \tau^{-1}, \quad (1)$$

where B is magnetic field, F is quantum oscillation frequency, and $\omega_c = eH/m^*c$, with m^* the cyclotron effective mass, is the cyclotron frequency. By this sub-

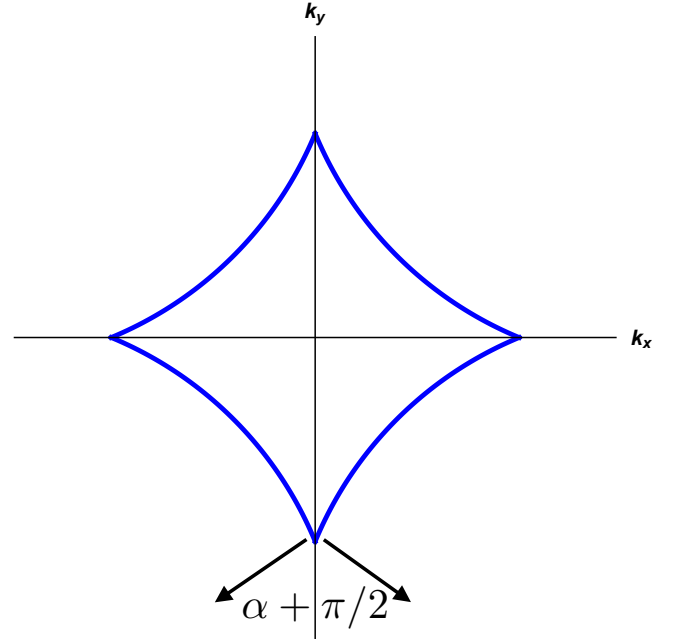


FIG. 1. Schematic diamond-shaped electron pocket Fermi surface, Ref. 1. This pocket is supposed to be centered around the nodal point $(k_x, k_y) = (\frac{\pi}{2}, \frac{\pi}{2})$ in the Brillouin zone. The lattice spacing is set to unity. When viewed as a part of a circle, each arc has a subtending angle α to the origin of that circle.

stitution they obtained quantum oscillations in the Hall coefficient with a single diamond-shaped electron pocket. As we explain below, it appears to have no justification for oscillations of R_H

In this Comment we raise some questions with regard to Ref. 1. On the issue of the sign of the Hall effect within the semiclassical approximation they make a large contribution to R_H , even though the vertices are a small portion of the Fermi surface,. One can describe a limiting process where one starts with a sufficiently smooth rounding of the Fermi surface. Manifestly R_H , especially in the large field limit, is simply the enclosed area, and not terribly sensitive to the shape. As the vertices get

more singular, the answer is non-generic. To summarize, unless there is some exchange of particles between multiple bands, or some balance of mobilities between different bands, it is hard to see how quantum oscillations of R_H could arise. We illustrate our argument with a simple two pocket model.

In the following we first show that in the small magnetic field limit, the Shockley-Chambers formula is consistent with the Jones-Zener formula⁷, regardless of how the sharp vertices in the Fermi surface contour are rounded. The sign of the small field Hall coefficient obtained in Ref. 1 heavily relies on a special rounding of the vertices. Different ways of rounding can lead to completely different conclusion about the sign, as correctly pointed out by N. P. Ong in Ref. 8. Therefore the conclusion of the sign reversal of R_H obtained in Ref. 1 is not convincing. Finally we explain why the simple replacement in Equation (1) to obtain quantum oscillations is physically inconsistent. We also give our reasonings why a pronounced quantum oscillation in a Hall coefficient is not expected for a single Fermi surface pocket. At the end we close our comment with some further discussions and conclusion.

II. SIGN OF R_H IN THE WEAK FIELD LIMIT

A. Shockley-Chambers formula and the Jones-Zener method in the weak field limit

The Shockley-Chambers formula for the 2D conductivity tensor $\sigma_{\alpha\beta}$ in a magnetic field is⁹

$$\sigma_{\alpha\beta} = \frac{1}{2\pi^2} \frac{e^2}{\hbar} \frac{m^* \omega_c}{\hbar} \int_0^{T_p} dt \int_0^\infty dt' v_\alpha(t) v_\beta(t+t') e^{-t'/\tau}, \quad (2)$$

where $\alpha, \beta = x, y$. In this formula the time variable t (or t') is introduced to parameterize an electron's semi-classical periodic cyclotron motion along the closed Fermi contour under the Lorentz force. $T_p \equiv 2\pi/\omega_c$ is the time period of one complete circuit motion. The Shockley-Chambers formula is a formal solution to the Boltzman equation in the presence of a perpendicular magnetic field and a longitudinal electric field. This formula itself is applicable in all field regimes, as far as the Landau level quantization effects can be neglected. When these effects are incorporated, there will be quantum corrections to the Shockley-Chambers formula, giving rise to quantum oscillations such as Shubnikov-de Haas effect.

Consider the weak field limit $\omega_c \tau \ll 1$. Then in Equation (2) we can expand

$$v_\beta(t+t') \approx v_\beta(t) + t' \frac{\partial v_\beta}{\partial t} \quad (3)$$

because the factor $e^{-t'/\tau}$ falls off very fast. On the right hand side the first term contributes a zero to the Hall conductivity σ_{xy} and therefore to the Hall coefficient R_H .

The second term gives a contribution $\propto B$ to σ_{xy} and therefore a magnetic field independent term to R_H as $R_H \propto \sigma_{xy}/B$. Higher order terms will give contributions $\sim \mathcal{O}(\omega_c \tau)$ or smaller to the Hall coefficient and therefore vanish in the limit $\omega_c \tau \rightarrow 0$. In other words in the zero magnetic field limit, the expansion in Equation (3) becomes exact. For σ_{xx} , keeping the first term in the expansion of Equation (3) is enough.

Substituting Equation (3) into Equation (2) leads to

$$\sigma_{xx} = \frac{1}{2\pi^2} \frac{e^2}{\hbar} \frac{m^* \omega_c \tau}{\hbar} \int_0^{T_p} v_x(t) v_x(t) dt, \quad (4)$$

$$\sigma_{xy} = \frac{1}{2\pi^2} \frac{e^2}{\hbar} \frac{m^* \omega_c \tau^2}{\hbar} \oint v_x(t) dv_y(t), \quad (5)$$

where the integration path \oint is along the closed Fermi surface contour. Using $\omega_c = eB/m^*c$ and the definition of the magnetic field length $l_B = \sqrt{\hbar c/eB}$ we can rewrite the Hall conductivity as

$$\sigma_{xy} = \frac{e^2}{h} \oint [v_x \tau] d[v_y \tau] / \pi l_B^2, \quad (6)$$

which is identical to the Jones-Zener method result, see Equation (4) of Ref. 8,

$$\sigma_{xy} = \frac{e^2}{h} \oint l_x dl_y / \pi l_B^2, \quad (7)$$

if we define a scattering path length vector: $\vec{l} = (l_x, l_y) = (v_x(t)\tau(t), v_y(t)\tau(t))$, as in Ref. 8. The assumption here is that $\tau(t) \equiv \tau$ is uniform along the Fermi surface contour.

Therefore within a uniform τ assumption, the small-field limit of Shockley-Chambers formula agrees perfectly with the Jones-Zener formula. Note that this conclusion does not depend on how the sharp vertices in the Fermi surface contour are rounded, contradicting the claim made in Ref. 1 that their consistency do depend on an appropriate rounding of the vertices.

B. Dependence of the sign of σ_{xy} on the variation of the Fermi velocity in the vicinity of the vertices

Although the consistency between the weak field limit Shockley-Chambers formula and the Jones-Zener formula does not depend on how the Fermi velocity around the sharp vertices are modeled, the sign of the computed $\sigma_{xy}(B \rightarrow 0)$ does depend on it crucially⁸. Therefore the sign of the $R_H(B \rightarrow 0)$ also heavily relies on the modeling of the Fermi velocity around the vertex. Different modeling can lead to opposite conclusions about the sign of $R_H(B \rightarrow 0)$.

1. The analysis of Banik and Overhauser

In Ref. 4, Banik and Overhauser defined the Fermi surface piece-wise manner by the four arc segments as in

Fig. 1, while neglecting any rounding effects at the vertices. Assuming that the magnitude of the Fermi velocity $|\vec{v}_F| = v_F$ is a constant along the Fermi surface contour, the Fermi velocity can be parameterised by

$$v_x(t) = v_F \cos \phi(t) \quad (8)$$

$$v_y(t) = v_F \sin \phi(t), \quad (9)$$

where

$$\begin{aligned} \phi(t) \equiv & \frac{4\alpha}{2\pi} \omega_c t - \left(\frac{\pi}{2} + \alpha\right) \sum_{n=1}^{n=4} \theta(\omega_c t - n\pi/2) \\ & + \left(\frac{\pi}{4} - \frac{\alpha}{2}\right) \end{aligned} \quad (10)$$

is the angle made by the Fermi velocity $\vec{v}_F(t) \equiv (v_x(t), v_y(t))$ with the x -axis at time t . On the right hand side the second term is a sum of four step functions, $\theta(x)$. These jumps of $\phi(t)$ at $\omega_c t = n\pi/2$ come from the “Bragg reflecton” of the particle at each vertex. The initial condition $\phi(t=0) = \frac{\pi}{4} - \frac{\alpha}{2}$ has been chosen such that the expression of $\phi(t)$ is simple. According to Equation (5), to calculate $\sigma_{xy}(B \rightarrow 0)$ we only need to compute $\tau^2 \oint v_x(t) dv_y(t)$. Because of the discontinuous jumps of $\vec{v}_F(t)$ at $\omega_c t = n\pi/2$ from one side of a vertex to the other, there is a nonzero contribution to the integral $\tau^2 \oint v_x(t) dv_y(t)$ from each vertex. In other words the integral can be decomposed into two parts as follows

$$\tau^2 \oint v_x(t) dv_y(t) \quad (11)$$

$$\begin{aligned} = & \tau^2 \left\{ \int_{a_1} + \int_{a_2} + \int_{a_3} + \int_{a_4} \right\} v_x dv_y \\ & - \tau^2 \sum_{n=1}^4 \delta_{\omega_c t, \frac{n\pi}{2}} v_x(t) \lim_{\delta \rightarrow 0} [v_y(t+\delta) - v_y(t-\delta)] \end{aligned} \quad (12)$$

$$\equiv A_a - A_d. \quad (13)$$

On the second line, $\int_{a_1}, \int_{a_2}, \int_{a_3}, \int_{a_4}$ stand for integrations along the four arc segments in Fig. 1. The sum of these four terms is denoted as A_a in the last line. The subscript “ a ” in A_a stands for “arc”. The third line is a sum of the discontinuous contributions of the Fermi velocity from the four vertices, as indicated by the Kronecker-delta $\delta_{\omega_c t, \frac{n\pi}{2}}$. This sum is then denoted as A_d in the last line, where the subscript d stands for “discontinuity”, stressing that it comes from the discontinuous jumps of the Fermi velocity.

A little inspection shows that A_a is equal to the sum of the Stokes area swept out by the scattering path vector \vec{l} as an electron moves along each Fermi arc segment. Therefore

$$A_a = 4 \frac{1}{2} \alpha (v_F \tau)^2 = 2\alpha l^2, \quad (14)$$

where $l = v_F \tau$ is the mean free path.

Computation of A_d is straightforward and the final result is

$$A_d = 2l^2 \cos \alpha. \quad (15)$$

Similar to A_a , A_d also has a geometric interpretation. This can be seen clearly if we anti-symmetrize $v_x(t)$ and $v_y(t)$ in calculating the Hall conductivity σ_{xy} . After the anti-symmetrization A_d can be rewritten as follows

$$\frac{A_d}{\tau^2} = \sum_{n=1}^4 \delta_{\omega_c t, \frac{n\pi}{2}} \frac{1}{2} [v_x(t) \Delta v_y(t) - v_y(t) \Delta v_x(t)], \quad (16)$$

where $\Delta v_{x/y}(t) = \lim_{\delta \rightarrow 0} [v_{x/y}(t+\delta) - v_{x/y}(t-\delta)]$. Now each term in the above sum can be identified as the area of the triangle made by the two Fermi velocity vectors on the two sides of each vertex. Each of them is equal to $\frac{1}{2} v_F^2 \sin(\frac{\pi}{2} + \alpha) = \frac{1}{2} v_F^2 \cos \alpha$. Therefore the sum is equal to $2v_F^2 \cos \alpha$ and $A_d = 2l^2 \cos \alpha$. Hence the Hall conductivity $\sigma_{xy} \propto (A_a - A_d) \propto (\alpha - \cos \alpha)$. Correspondingly the Hall coefficient $R_H \propto (\alpha - \cos \alpha)$. So it changes sign as α changes from $\pi/2$ to 0.

From this analysis we see that the small field Hall conductivity contains not only a contribution A_a from each arc segment, but also another contribution A_d from the discontinuous jumps of the Fermi velocity from one arc to the adjacent arc at each vertex. We should emphasize that this A_d contribution exists without taking into account how the vertices are rounded.

2. Harrison and Sebastian rounding of the vertices

After computing the σ_{xy} directly from the Shockley-Chambers formula, the authors of Ref. 1 then tried to calculate the σ_{xy} by computing the Stokes area swept out by the scattering path vector as an electron moves along the entire Fermi surface contour, following N. P. Ong⁸. There are two contributions: one from the four disjoint arc segments; the other from the vicinity of vertices. The arc segment contribution is equal to A_a as computed in the previous section and given by Equation (14). Computing the vertex contributions requires a knowledge of how the sharp vertices are rounded and how the Fermi velocity varies near the vertices after rounding. We denote this contribution as A_v , where the subscript “ v ” stands for vertices.

In order to compute A_v the authors of Ref. 1 modeled the vertices by assuming an elastic Bragg reflection of quasiparticles at the end of the disconnected Fermi arcs from the charge density wave (CDW). However, this is hardly justified without a real understanding of the nature of the Fermi arcs and also the semi-classical dynamics of the quasiparticles at the end of the Fermi arcs before the reconstruction takes place. Using this modeling of the vertices the authors of Ref. 1 then calculated the vertex contribution A_v .

The surprising thing is that the A_v they have obtained is identical to A_d introduced in the previous section, which comes from the discontinuous jump of the Fermi velocity at the vertices without rounding. Therefore the $\sigma_{xy} \propto A_a - A_v$ calculated in Ref. 1 is identical to the

$\sigma_{xy} \propto A_v - A_d$ computed in the previous section by following Banik and Overhauser. Based on this fact the authors of Ref. 1 have claimed that such an agreement shows that they have appropriately modeled the variation of the Fermi velocity in the vicinity of vertices using Ref. 4 to compute the σ_{xy} . But from our analysis we see that this claim cannot be true. The agreement between A_v and A_d they have found is a coincidence, not generic. A different way of rounding the vertices can give a contribution A_v that is completely different from A_d in general (see, for example, Ref. 8).

This can be a big concern especially given that the experimentally observed CDW in the cuprates has a very short in-plane correlation length (see, for example, Ref. 10), which would likely smear out any details of an elastic Bragg scattering in the small vertex region, even if the Bragg scattering of quasiparticles on the Fermi arcs were to be well defined.

In short, the sign of the small field σ_{xy} depends on how the sharp vertices are rounded. The special modeling of the vertices in Ref. 1 might be artificial. Therefore it puts the conclusion obtained about the sign of the small field σ_{xy} in doubt. A slightly more realistic modeling of the Fermi velocity around the vertices might change the final results.

III. QUANTUM OSCILLATION CORRECTIONS AT HIGHER MAGNETIC FIELDS

In the following we first give our reasons why a simple replacement of τ with $\tilde{\tau}$ in the Shockley-Chambers formula to extract quantum oscillation is wrong and also give our arguments as to why multiple pocket scenario is reasonable.

A. Inconsistency of the replacement of τ^{-1} with $\tilde{\tau}^{-1}$ in Shockley-Chambers formula

To obtain quantum oscillations in the Hall coefficient the authors in Ref. 1 made a simple substitution of the mean free time τ in Eq. (1) into the Shockley-Chambers formula in Eq. (2). However this kind of treatment can not be correct. We know that the Shockley-Chambers formula is a formal solution to the semi-classical Boltzmann equation in the presence of both an electric field \vec{E} and a perpendicular magnetic field \vec{H}

$$(-e)\vec{E} \cdot \vec{v}_{\vec{k}} \frac{\partial f^0}{\partial \epsilon} + \frac{-e}{\hbar c} \vec{v}_{\vec{k}} \times \vec{H} \cdot \nabla_{\vec{k}} g = \frac{g}{\tau}, \quad (17)$$

where f^0 is the equilibrium distribution in the absence of fields \vec{E}, \vec{H} and g is the out of equilibrium distribution due to the fields. The total distribution is $f = f^0 + g$. The right hand side of this equation accounts for the relaxation back to the equilibrium distribution due to incoherent scattering processes within the relaxation time

approximation. However, the *ad hoc* replacement¹ of τ by $\tilde{\tau}$ in Eq. 1 cannot be used to calculate the Hall coefficient R_H . This is because the Hall coefficient is geometric and does not directly depend on τ^{-1} ; see Ref. 8.

B. Arguments favoring quantum oscillations of Hall coefficient in the multiple pocket scenario

In the extreme high field limit neither single nor the multiple pocket scenario can lead to quantum oscillations. However, for the experimentally accessed field range the situation strongly favors the multiple pocket scenario.

Consider a simple two pocket situation of longitudinal resistivities ρ_1 and ρ_2 and the corresponding Hall coefficients R_1 and R_2 . A well known result¹¹ for $R(H)$ is

$$R(H) = \frac{\rho_2^2 R_1 + \rho_1^2 R_2 + R_1 R_2 (R_1 + R_2) H^2}{(\rho_1 + \rho_2)^2 + (R_1 + R_2)^2 H^2} \quad (18)$$

In general, for values of the magnetic field as in the current experiments, the differing ρ_1 , ρ_2 , R_1 , and R_2 can give rise to quantum oscillations because the scattering rates do not cancel out from the numerator and the denominator, as can be easily seen. However, if we consider $H \rightarrow \infty$,

$$R(H) \rightarrow \frac{R_1 R_2}{(R_1 + R_2)}, \quad (19)$$

which is independent of H ; hence no quantum oscillations. Whether this limit is attained or not can be seen in future experiments. It would imply decreasing quantum oscillation of Hall amplitudes with field, as the higher field regime is approached. This would be interesting to observe in future experiments.

IV. CONCLUSION

The conclusion about the sign of the zero field Hall conductivity/coefficient obtained in Ref. 1 heavily relies on a special modeling of the sharp vertices in the diamond-shaped electron pocket Fermi surface of Fig. 1 and is therefore non-generic. The quantum oscillation in the Hall coefficient obtained in Ref. 1 was based on an inconsistent substitution of the mean free time with an oscillatory mean free time in the Shockley-Chambers conductivity formula. We have given arguments disfavoring this treatment.

The negative Hall coefficient is quite a general result in the cuprates. Even in cuprates where it's not negative at higher temperatures, it heads towards negative values at low temperatures. The specifics of the CDW, on the other hand, vary quite a bit between different cuprates. And one could imagine that the details of the rounding of the corners would be very different indeed. Therefore it seems unlikely that something so general-negative Hall

coefficient-could rely on something so specific as corner rounding.

Experimentally, there is an observation of small electronic specific heat coefficient¹² proportional to \sqrt{H} , which is hard to reconcile with the multiple pocket scenario. However, this experiment is still controversial; see, Ref. 13, There are, however, other experiments, such as those in Refs. 14 and 15, which favor multiple pockets scenario. In addition, in a recent direct experiment a second small hole pocket is indeed observed in quantum oscillation measurements in cuprates¹⁶ consistent with the multiple pocket scenario.

ACKNOWLEDGMENTS

We thank Ching-Kit Chan, S. Kivelson, B. J. Ramshaw and I. Vishik for many discussions. This work was partly performed at the Aspen Center for Physics, which is supported by National Science Foundation grant PHY – 1066293. It was also supported in part by the funds from the David S. Saxon Presidential Term Chair at UCLA.

-
- ¹ N. Harrison and S. E. Sebastian, Phys. Rev. B **92**, 224505 (2015).
 - ² W. Shockley, Phys. Rev. **79**, 191 (1950).
 - ³ R. G. Chambers, Proceedings of the Physical Society. Section A **65**, 458 (1952).
 - ⁴ N. C. Banik and A. W. Overhauser, Phys. Rev. B **18**, 1521 (1978).
 - ⁵ D. LeBoeuf, N. Doiron-Leyraud, J. Levallois, R. Daou, J. B. Bonnemaïson, N. E. Hussey, L. Balicas, B. J. Ramshaw, R. Liang, D. A. Bonn, W. N. Hardy, S. Adachi, C. Proust, and L. Taillefer, Nature **450**, 533 (2007).
 - ⁶ N. Doiron-Leyraud, C. Proust, D. LeBoeuf, J. Levallois, J.-B. Bonnemaïson, R. Liang, D. A. Bonn, W. N. Hardy, and L. Taillefer, Nature **447**, 565 (2007).
 - ⁷ H. Jones and C. Zener, Proceedings of the Royal Society of London A: Mathematical, Physical and Engineering Sciences **145**, 268 (1934).
 - ⁸ N. P. Ong, Phys. Rev. B **43**, 193 (1991).
 - ⁹ J. M. Ziman, *Principles of The Theory of Solids*, 2nd ed. (Cambridge University Press, 1972).
 - ¹⁰ J. Chang, E. Blackburn, A. Holmes, N. Christensen, J. Larsen, J. Mesot, R. Liang, D. Bonn, W. Hardy, A. Watenphul, M. Zimmermann, E. Forgan, and S. Hayden, Nature Physics **8**, 871 (2012).
 - ¹¹ N. W. Ashcroft and N. D. Mermin, *Solid State Physics* (Thomson Learning, 1976).
 - ¹² S. C. Riggs, O. Vafek, J. Kemper, J. Betts, A. Migliori, F. Balakirev, W. Hardy, R. Liang, D. Bonn, and G. Boebinger, Nature Physics **7**, 332 (2011).
 - ¹³ C. Marcenat, A. Demuer, K. Beauvois, B. Michon, A. Grockowiak, R. Liang, W. Hardy, D. Bonn, and T. Klein, Nature communications **6**, 7927 (2015).
 - ¹⁴ P. M. C. Rourke, A. F. Bangura, C. Proust, J. Levallois, N. Doiron-Leyraud, D. LeBoeuf, L. Taillefer, S. Adachi, M. L. Sutherland, and N. E. Hussey, Phys. Rev. B **82**, 020514 (2010).
 - ¹⁵ C. Proust, B. Vignolle, J. Levallois, S. Adachi, and N. E. Hussey, Proceedings of the National Academy of Sciences **113**, 13654 (2016).
 - ¹⁶ N. Doiron-Leyraud, S. Badoux, S. R. De Cotret, S. Lepault, D. LeBoeuf, F. Laliberté, E. Hassinger, B. J. Ramshaw, D. A. Bonn, W. N. Hardy, R. Liang, J.-H. Park, D. Vignolles, B. Vignolle, L. Taillefer, and C. Proust, Nature communications **6**, 6034 (2015).